▼ Journal of Research (Science), Bahauddin Zakariya University, Multan, Pakistan.
Vol.17, No.1, January 2006, pp. 59-72 ISSN 1021-1012

# NOVEL TECHNIQUES FOR CHARACTERIZATION AND KINETICS STUDIES OF Bi-2223 CONDUCTORS

M. N. Khan[1] and Kh. Zakaullah[2]
[1]Bahauddin Zakariya University, Multan. [2]GIK Institute of Engineering Sciences & Technology Topi, District Swabi, NWFP, Pakistan.
email: zaka@giki.edu.pk

**Abstract:** The Bi-2223 high temperature superconductor (HTS) powder-in-tube (PIT) tape and long-lengths of conductors with unique performance has provided the ability to construct a wide range of HTS electric power components. Oxygen doping, cation doping, phase transition and strain all strongly influence the superconducting transition temperature $T_c$. We report to characterize these materials by thermal analysis, X-ray diffraction and scanning electron microscopy. Activation energies and frequency factors employing different models were evaluated. It was observed that both peritectic transition and reaction rates were dependent on ambient atmosphere. X-ray diffraction results showed that volume fraction of the high-$T_c$ (2223) phase decreases and that of low-$T_c$ (2212) phase increases with the increase of rare-earth ion content. SEM studies revealed that the conversion of 2212 pre-cursor phase to 2223 was significantly influenced by the sintering atmosphere and the lower partial pressure of $O_2$ which promoted faster conversion of 2212 phase and smaller 2223 grain size. The critical current densities of silver sheathed tapes using the powder-in-tube were found to be in the range 7 x $10^8$ A $m^{-2}$. A possible explanation for the difference in phase transformation and the effects on the critical current was discussed.

**Keywords:** Bi-2223, characterization techniques, doping, reaction kinetics, superconductors.

## INTRODUCTION

Superconductivity has fascinated the imagination of scientists, engineers and technologists because of its unusual nature and immense potentialities. NMR imaging and many other electronic and magnetic devices have been fabricated using materials, which attain superconductivity at liquid helium temperature. The first discovery [Wu *et al*. 1987] of a material that could superconduct at a temperature greater than the boiling point of liquid nitrogen reinvigorated the interest in the use of superconductors in power technology.

The (Bi, Pb)-2223 phase formation strongly depends on parameters such as sintering temperature, thermal processing time, synthesis atmosphere, precursor compositions and doping or substituting various cations and anions [Marty *et al.* 1998, Watanab and Kojima 1998, Azzouz *et al*. 2001]. Research is being carried out to make new materials which are superconducting at high temperatures. Superconductivity is an emerging technology for high performance electronics. It offers unique and beneficial attributes for sensor, signal processing, and communication systems. Yet, industry faces technical hurdles and market obstacles to identify business targets. Our ability to define and achieve successful paths which overcome the technical and market barriers will determine the viability of superconductivity in the electronic industry, and coincidentally that of applied research in this technology.

Long length of bismuth (BSCCO-2223) superconductor wires are used for the prototype products. The wires are fabricated by the powder-in-tube (PIT) technique: the superconductor pre-cursor powder is packed in pure silver or silver alloy tubes and mechanically deformed by wire drawing and rolling to produce long lengths of wires. The wires are thermally treated to convert them into superconductors.

We have made a systematic investigation of phase characterization and $J_c$ studies [Khan *et al*. 1994, 1998, 2001, Khan and Khizar 1999, Zakaullah *et al*. 2005] for $Bi_2Sr_2Ca_2Cu_3O_{10}$ (BSCCO) in both wire and bulk forms. This paper reviews some of the recent advances in processing and characterizing of Bi-based superconductors.

## RECENT DEVELOPMENTS

Over the last 10 years an intense research effort has led to the developments of Ag-sheathed $(Bi, Pb)_2Sr_2Ca_2Cu_3O_{10=d}$ tapes with increasingly promising performances and confirmed the reliability of this material in HTSC technological applications. However, details of the high-temperature mechanism that could explain the still unknown aspects of the Bi,Pb(2223) phase formation have only been investigated in the most recent past. The mechanism leading to the conversion of the precursor powders in to the phase Bi, Pb (2223), as well as the all the secondary phases present were studied using XRD analysis and both SEM and TEM characterization. Advances in processing and fabrication of high critical current density ($J_c$) long length conductors, silver sheathed super-conducting magnets and coils from silver sheathed Bi-2223 tapes, pancake coil magnets from 1 to 10 m length and mono-multifilament Bi-2223/2212 high $T_c$ superconductors by powder technique continue to bring these materials closer to commercial applications.

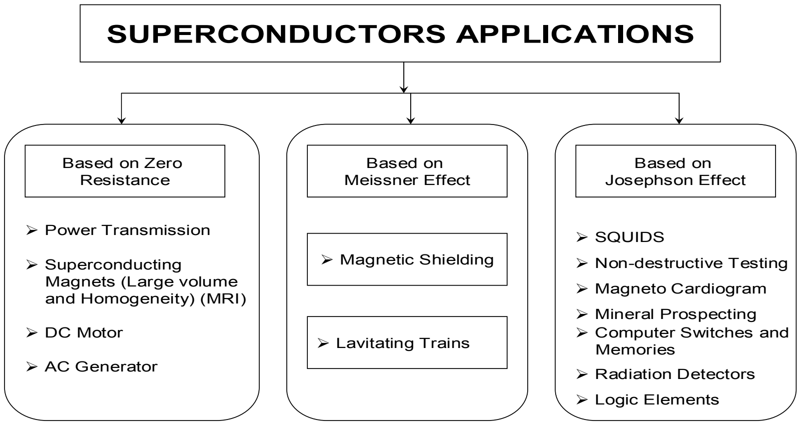

## PROBLEMS

Fabrication of high-$J_c$, long-length conductors is essential for successful application of high $T_c$ superconductors. Several different approaches for high-Jc, wire fabrications have been demonstrated, however, none of them meets all the requirements in terms of desirable length, critical currents, and operating temperature ranges. High $J_c$ YBCO wires have been made only in length less than a meter. The BSCCO wires / ribbons exhibit high $J_c$ and can be made long but they are not particularly useful for major applications above ~30K. For TBCCO, neither high $J_c$ long wire comparable to BSCCO material nor sufficient flux pinning, comparable to YBCO has been demonstrated, even with the promising single TI-O layered compound.

The main problem hindering the study of chemical reactions inside the silver sheath comes from the cladding itself. Because of the strong X-ray absorption in silver conventional low energy XRD measurements (~8KeV for CuKα radiation) performed at room temperature can only be made after removal of Ag sheath.

## WHY THIS WORK?

Polycrystalline bulk superconductors usually have a low critical current density $J_c$ and this has been explained due to the so-called weak coupling of grains. It has been demonstrated that addition of silver to YBCO and BSCCO superconductors improves their critical current densities without adversely affecting their superconducting properties. It has been claimed that Ag atoms do not enter the lattice of BSCCO superconductors but appear to have filled up the voids partially between individual superconducting grains by preferential segregation. It is also known that the silver addition in the BSCCO system does not alter the formation a structure of 100K phase. Some investigators have observed that silver enhanced flux pinning in the inter-granular region with optimum current density at 20-30 vol. % Ag.

## MATERIALS AND METHODS

A solid-state reaction scheme was chosen for the powder synthesis. $Bi_2O_3$, PbO, $SrCO_3$, $CaCO_3$ and CuO were prepared by decomposition of metal nitrate solution in the cation ratio $Bi_{1.72}Pb_{0.3}Sr_2Ca_{2-x}Nb_xCu_3O_y$. The powders were calcined at 820°C for 10h, uniaxially pressed into pellets, and sintered at 840°C for different times in order to alter the phase assemblage. It was found that nitrate solution route provided highly reactive, homogenous and carbonate-free powders from which the 2223 phase can be formed effectively. It should be however, pointed out that at this stage the powders contain a small fraction of the 2223 and the 2212 is the major phase. This incompletely reacted precursor will facilitate the liquid phase formation in the subsequent processes. The average particle size was 2 to 3 μm temperature in the furnace.

## CHARACTERIZATION TECHNIQUES

Differential thermal analysis (DTA) was carried out in various atmospheres at different heating rates using a Perkins Elmer DSC–7. The kinetics of crystallization of the samples was investigated from non-isothermal DTA using a Perkin Elmer DTA–7 at a heating rate of 5–20°C min$^{-1}$. Glass samples were annealed in air for various lengths of time at temperatures selected from the DTA results. Crystalline phases formed in the annealed specimens were identified from the powder XRD patterns, which were recorded at room temperature. The electrical resistance was measured from 77 to 160 K by the standard four-probe configuration with 1.0 µV cm$^{-1}$ used as the criteria for $J_c$ measurements.

Bi-2223 conductors doped with Nb, Sm, Tb and Ag were prepared by the heat treatment of rapidly quenched glass precursors. Activation energies and frequency factors, employing different models were evaluated. It was observed that both peritectic transition and reaction rates were dependent on ambient atmosphere. The resistivity measurements revealed that the critical temperature decreases with increasing Nb, Sm, Tb and Ag concentration. The critical current density Jc measured at 77K from I-V data shows an increase with silver addition. The critical current densities of silver sheathed tapes using the powder-in-tube were found to be in the range 7x108Am-2. X-ray diffraction results showed that the volume fraction of the high-Tc (2223) phase decreases and that of low-Tc (2212) phase increases with increase of these rare-earth ion contents. These results are explained on the basis of possible variation of hole concentration with trivalent rare-earth ion substitution and also by considering the magnetic nature of the substituted ion in the composition.

Bi-2223 tapes were made using powder-in-tube technology. They consisted of a thin strip-shaped silver or silver alloy matrix containing many flat filaments of Bi-2223 superconductor. Typical overall dimensions were 3-4 mm wide and 0.25–0.35 mm thick. The metal sheath supports the ceramic Bi-2223 filaments and acts as a resistive shunt in the case of fault currents exceeding the tape critical current. Tapes with silver-alloys provide higher strength or lower thermal conductivity.

## TAPE SPECIFICATIONS FOR POWER CABLES

The quantity $J_c$ equal to the macroscopic critical current ($I_c$) divided by the total cross-sectional area of the Bi-2223, is normally used to characterize tapes. With multi-filamentary tapes the area cannot be accurately measured and a more useful quantity for application design is the engineering current density, $J_E$, equal to $I_c$ divided by the cross-sectional area of the whole tape (metal sheath and Bi-2223). The $J_E$ of these tapes is usually 20-30% of the $J_c$.

The main conclusions on the properties of the superconducting materials that would be needed for commercial products are:

### i) Length and Handling Properties

The superconducting wire or tape must be made in lengths of > 1km. To avoid degradation of the superconducting properties during cabling the metal sheath must have a high tensile strength.

### ii) Operating Temperature

If a cable is to be cooled by liquid nitrogen (currently the only economic solution) there will be temperature gradients along its length. The tapes may have to meet the required specification temperatures above 77K.

### iii) Current Density

The magnitude of the engineering current density ($J_E$) depends on the cost of material fabrication and the type of cable. It should range from 1-3 x $l0^8$ A $m^{-2}$.

### iv) Operating Fields

It is estimated that the self-fields in a cable could be as much as 0.2 T. Unfortunately the Jc of Bi-2223 is greatly reduced in only small fields perpendicular to the tape surface at 77 K. Careful design can minimize this self-field component as long as there is a homogenous current distribution throughout the cable. This requires good control of Jc variations along the tape lengths.

### v) AC Loss

For ac cables the loss in each phase should be less than 1W $m^{-1}$. Existing Bi-2223 tapes are good enough for fabricating cable prototypes so that experience of some of the many engineering problems can be gained.

## RESULTS AND DISCUSSION

Fig. 1 shows XRD pattern of bismuth family of superconductors. Orthorhombic lattice cell parameters were calculated and are presented in Table 1.

**Table 1:** Lattice Parameters of Orthorhombic Phases of Bismuth Family of Superconductors.

| System | a (Å) | b (Å) | c (Å) | $T_{c\text{- zero}}$ (K) |
|---|---|---|---|---|
| 2201 | 5.375 | 5.310 | 24.525 | - |
| 2212 | 5.230 | 5.412 | 29.180 | 77 |
| 2223 | 5.218 | 5.632 | 30.815 | 100 |

Fig. 2 shows the x-ray diffraction patterns of the undoped (x = 0) and Sm, Tb doped (x=1) samples annealed at 850oC for 240 hours, which revealed various phases present in the crystalline samples. A good agreement both in lattice parameters and intensity ratios of the high $T_c$ and low $T_c$ peaks was found with those reported in the literature. Fig. 2 suggests that for undoped samples (x = 0) the number and intensities of high $T_c$ phase reflections are predominant compared to the low $T_c$ phase reflections.

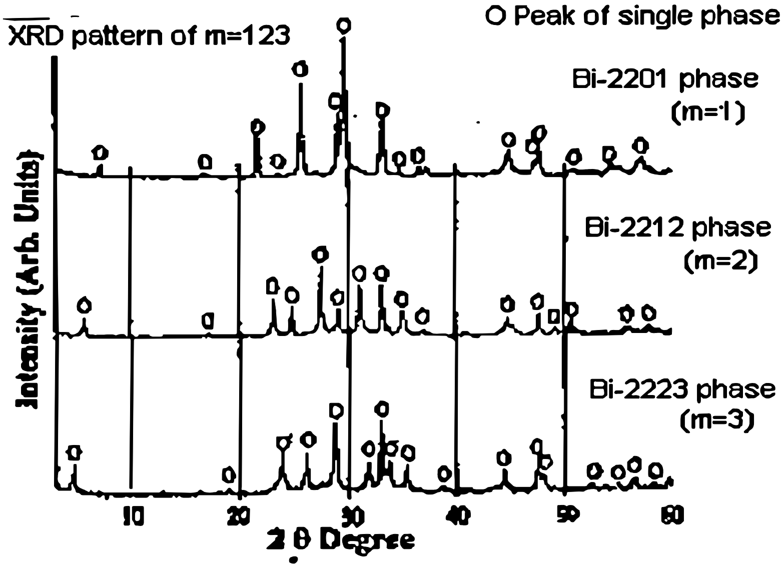

**Fig. 1:** XRD patterns of Bi-family of superconductors (a) 2223 phase, (b) 2212 Phase and (c) 2201 phase.

The relative volume fractions of high Tc and low Tc phases were determined by using the following well known expressions [Khan and Khizar 1999] and are given in Table 2.

$$f_{2223} = \frac{I_{2223}(hkl)}{I_{2223}(hkl) + I_{2212}(hkl)}$$

$$f_{2212} = \frac{I_{2212}(hkl)}{I_{2212}(hkl) + I_{2223}(hkl)}$$

It was observed that for undoped samples (x = 0) the volume fraction of high $T_c$ phase is maximum (91.6%) with very small amount of 2212 phase present (8.3%). The volume fraction of 2223 phase decreases and that of 2212 phase increases for the samples doped with Sm and Tb.

**Table 2:** Volume fraction of high $T_c$ (2223) and low $T_c$ (2212) phases of undoped and doped BSCCO samples.

| Composition | Volume Fraction (%) | |
|---|---|---|
| | 2223 Phase | 2212 Phase |
| BSCCO | 91.6 | 08.3 |
| BSSmCCO | 37.7 | 62.2 |
| BSTbCCO | 50.0 | 50.0 |

Fig. 3 shows x-ray diffraction patterns of the undoped (with x = 0) samples annealed at 850 °C for 25 hrs and 240 hrs in air for 2θ ranging up to 70°. The intensity and peak positions of the (0 0 2), (0 0 1 0), (1 1 5) (1 0 9), (0 0 1 2), (1 1 9), (2 0 0) and (0 0 1 4) reflections are in good agreement with the values reported in literature for high $T_c$ 2223 phase. It

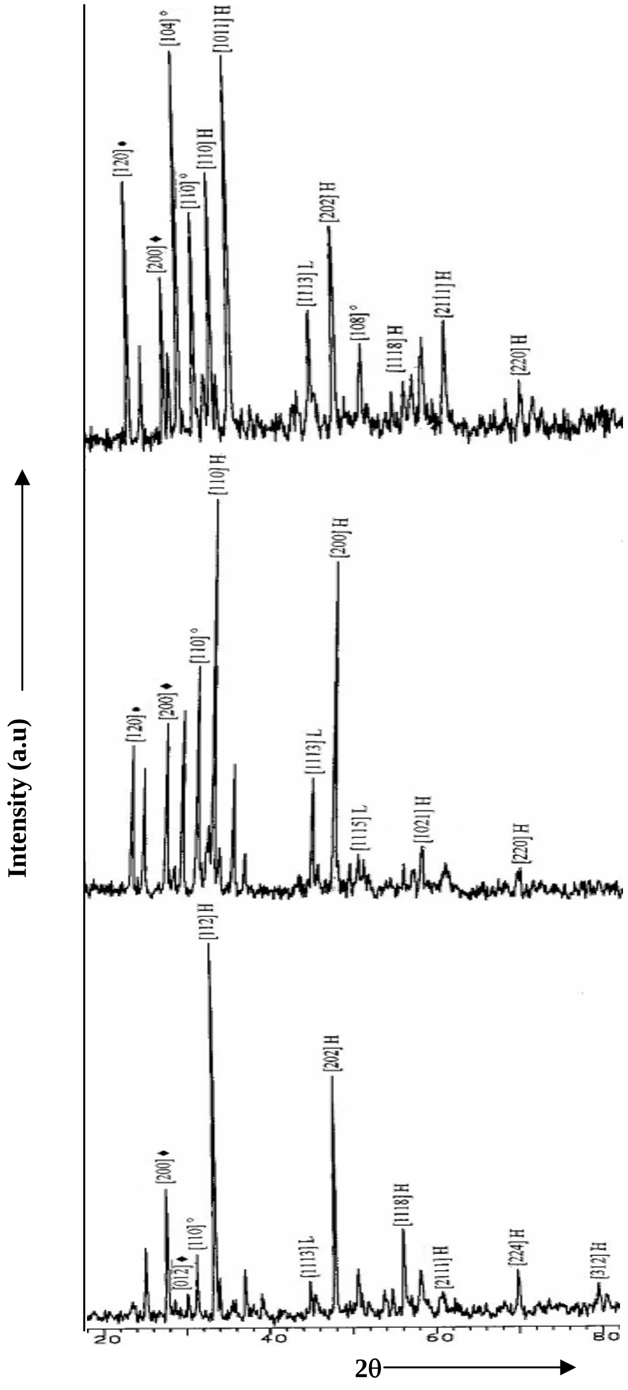

**Fig. 2:** XRD reflections of undoped, Sm doped and Tb doped BSCCO samples. H – 2223 phase, L – 2212 phase, ♦ – $Pb_2O_3$, • – $Ca_2PbO_4$, ° – $CaPbO_3$.

is evident from Fig. 3 that the intensity of reflections corresponding to high-$T_c$ phases increased and those corresponding to low $T_c$ phases decreased with increasing sintering time. The 'c' value of high-$T_c$ phase is 38 Å and that of low-$T_c$ phase is 31 Å. The peaks at 2θ = 4.4° and 4.6° correspond to (0 0 2) reflections of high- and low-$T_c$ phases respectively.

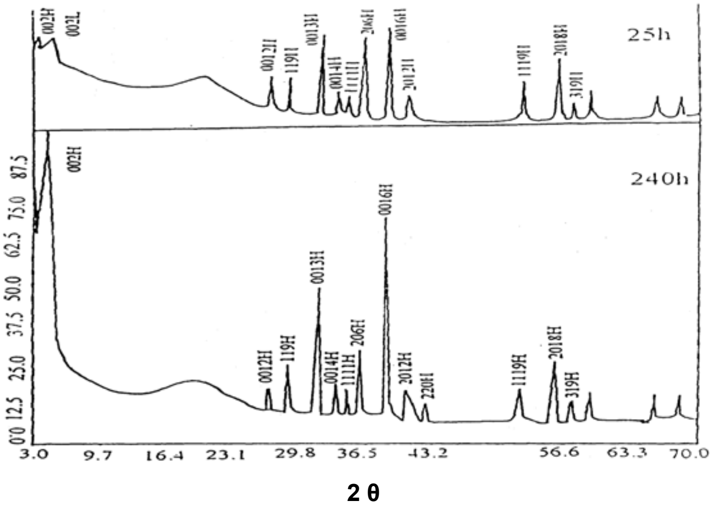

The peaks denoted by (H) and (L) correspond to High $T_c$ (2223) and Low $T_c$ (2212) phases respectively.

**Fig. 3:** XRD patterns for $Bi_{1.65}Pb_{0.32}Ag_xSr_{1.73}Ca_{1.33}Cu_{3.85}O_y$ superconductor with A = 25hrs, B = 240hrs.

In the sample sintered for 25 hrs, distinct peaks at 2θ = 4.4° and 4.6° appeared indicating that the sample consisted of both low- and high- $T_c$ phases. With increasing sintering time one can notice gradual increase in the intensity of the peak at 2θ = 4.4° corresponding to (0 0 2) reflection of the high- $T_c$ phase with a decrease in the intensity of peak at 2θ = 4.6°. For the sample sintered for 240 hrs the low- Tc phase peak at 2θ = 4.6° is almost absent and peaks corresponding to the high-$T_c$ phase are relatively sharper. These results indicate that on heating the glass $Bi_2Sr_2Ca_0Cu_1O_8$ (2201) phase crystallizes out first followed by the formation of 80K $Bi_2Sr_2Ca_1Cu_2O_8$ (2212) phase at the higher temperature. The 110K $T_c$ phase is formed at still higher temperature just below the melting point, probably by reaction between the low-$T_c$ 2201 phases. We obtained the values of lattice constants a=5.60 Å, b=5.20 Å and c=37.75 Å. The lattice constants for the sample annealed for 25 hrs are a=5.39 Å, b=5.51 Å and c=30.82 Å. This confirmed that the high-$T_c$ (2223) and low-$T_c$ (2212) phases differ mainly in the length of c-axis.

Resistivity of bulk samples, measured using van der Pauw's four-probe method, are shown in Fig. 4. Helium cooled closed cycle cryostat was used for resistivity measurements up to 15 K, for 2212 and 2223 phases. Metallic behavior and sharp transitions at 77 K for 2212 and 99 K for 2223 were observed.

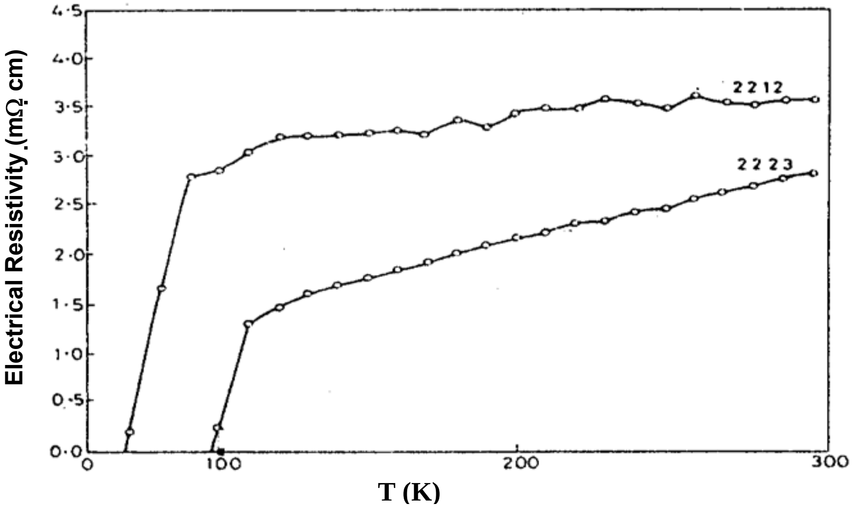

**Fig. 4:** Electrical resistivity plots for 2212 and 2223 phases.

We summarize the crystallization mechanism in the interior of the $Bi_2Sr_2CaCu_2O_x$ glass during annealing as follows.

$$\text{Glass} \xrightarrow{780^\circ C} Bi_2Sr_{3-x}Ca_xO_y\ (x=1) + Cu_2O + Bi_2Sr_2CuO_x$$

$$\xrightarrow{780^\circ C} \text{Melt} \xrightarrow{>780^\circ C} Bi_2Sr_2CaCu_2O_x$$

A typical DSC scan of $Bi_{1.6}Pb_{0.4}Sr_{1.7}Ca_{2.3}Cu_3O_y$ glass showing the glass transition ($T_g$) and crystallization temperatures ($T_x$) is depicted in Fig. 5.

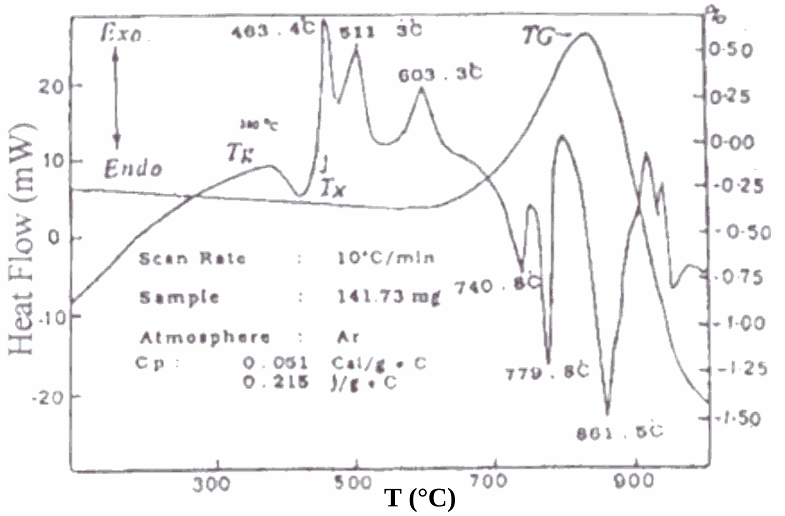

**Fig. 5:** A typical scan of $(Bi_{1.6}Pb_{0.4})Sr_{1.7}Ca_{2.3}Ag_xCu_3O_y$ glass in Argon atmosphere at heating rate of 10°C min$^{-1}$.

The $T_g$ and $T_x$ temperatures for this system are 379.77°C and 463.40°C respectively. Several other exothermic and endothermic peaks are also observed at temperatures above $T_x$. A $T_g$ curve in air for the bulk sample is also shown in Fig. 5. It is clear that increase in weight is very gradual and the maximum increase occurs at above 813°C. These results indicate that the diffusion of oxygen into the interior of the sample at temperatures below around 600°C was very slow. We noted that the endothermic peak appeared at 779.8°C in the bulk sample. It is of particular interest to clarify the origin of this endothermic peak because the $Bi_2Sr_2Ca_2Cu_3O_x$ phase precipitates and grows at above this endothermic temperature. It is clear that the reaction among the $Bi_2Sr_{3-x}Ca_xO_y$(x = 1), $Cu_2O$ and $Bi_2Sr_2CuO_x$ phases in the interior of the sample is closely related at around 779.8°C. We summarize the crystallization mechanism as follows: the 2201 phase first precipitates out followed by the formation of 2212 phase at higher temperatures. The 110 K $T_c$ phase is formed at 861.5°C just below the melting point, probably by reaction between the low- $T_c$ 2201 and 2212 phases and the residual calcium and copper oxides.

Values of kinetic parameters were calculated using the kinetic model [Bansal and Doremus 1984], which is expressed as:

$$ln\left|\frac{T_p^2}{\alpha}\right| = ln\left|\frac{E}{R}\right| - ln\,\nu + \frac{E}{R\,T_p} \qquad (1)$$

Where $T_p$ is the peak maximum temperature in the DSC and $\alpha$ the heating rate. Eq. (1) is an expression of the Johnson-Mehl-Avarmi isothermal kinetic model for use in non-isothermal methods. In the derivation of Eq. (1), it has been assumed that the rate of reaction is maximum at the peak, which is valid for power-compensated DSC. For each of the four peaks observed in the DSC traces, peak temperatures were determined and the plots of $ln\left|\frac{T_p^2}{\alpha}\right| Vs.\left[\frac{1}{T_p}\right]$ are presented in Fig. 6. All the plots are linear indicating the applicability of the Bansal-Doremus model [1984].

From the linear least-square fitting of the data, values of the kinetic parameters such as activation energy and Avrami's exponent were calculated and are given in Table 3.

**Table 3:** Kinetics Parameters for BSCCO samples derived from Bansal - Dormus model.

| Sr. No. | Composition | Kinetic Parameters by Bansal's Equation | | | Avrami Exponent (n) |
|---|---|---|---|---|---|
| | | Activation Energy (kJ mol$^{-1}$) | Frequency factor (sec$^{-1}$) | K value | |
| 1 | $Bi_{1.7}Pb_{0.3}Sr_2Ca_2Cu_3O_y$ | 252.26 | 1.80 x 1017 | 0.2700 | 1.58 |
| 2 | $Bi_{1.7}Pb_{0.3}Sr_2Ca_{1.95}Sm_{0.1}Cu_3O_7$ | 255.79 | 1.10 x 1018 | 0.5500 | 1.62 |
| 3 | $Bi_{1.7}Pb_{0.3}Sr_2Ca_{1.95}Sm_{0.75}Cu_3O_7$ | 275.01 | 3.20 x 1019 | 0.8500 | 1.67 |
| 4 | $Bi_{1.6}Pb_{0.4}Sr_2Ca_2Cu_3O_y$ | 410.50 | 1.10 x 1027 | 0.0141 | --- |
| 5 | $Bi_{1.6}Pb_{0.4}Sr_2Sm_1Ca_2Cu_3O_y$ | 246.22 | 1.07 x 1015 | 0.0087 | --- |
| 6 | $Bi_{1.6}Pb_{0.4}Sr_2Tb_1Ca_2Cu_3O_y$ | 236.48 | 8.05 x 1013 | 0.0079 | --- |

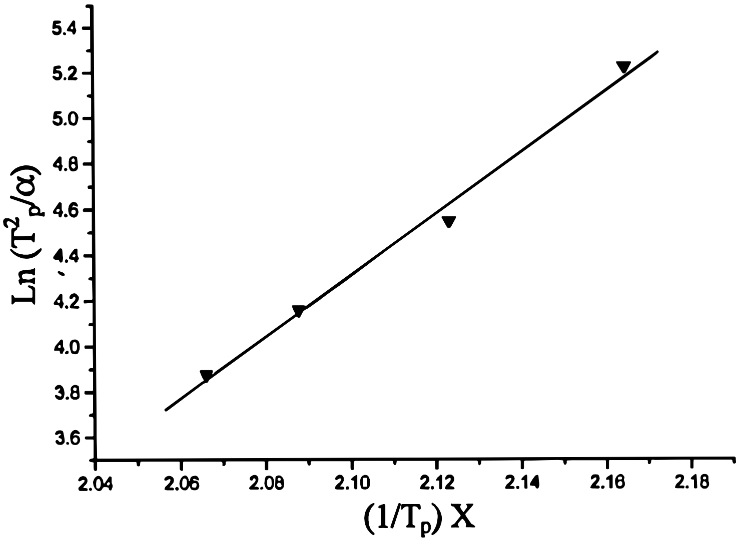

**Fig. 6:** A plot of $ln\left|\frac{T_p^2}{\alpha}\right| Vs.\left[\frac{1}{T_p}\right]$ for the niobium- doped sample.

Another typical DSC scan of $(Bi_{1.6}Pb_{0.4})Sr_{1.7}Ca_{2.3}Cu_{2.3}O_y$ glass showing the glass transition ($T_g$) and crystallization temperature ($T_x$) is depicted in Fig. 7.

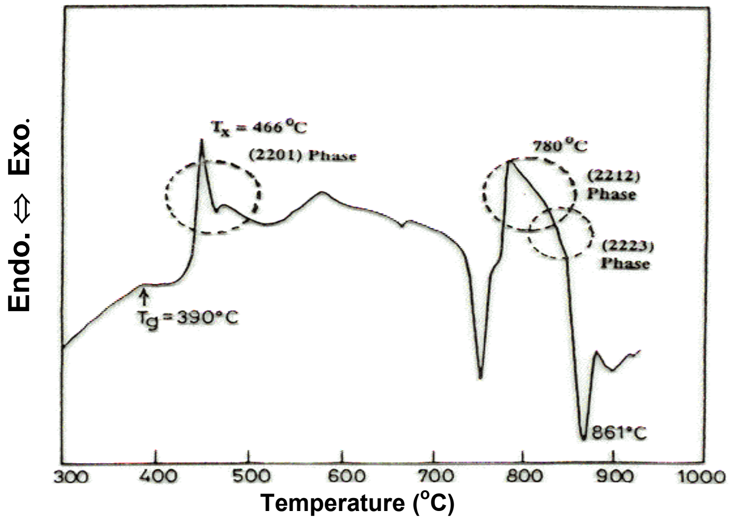

**Fig. 7:** Differential Thermal Analysis of $(Bi_{1.6}Pb_{0.4})Sr_{1.7}Ca_{2.3}Cu_3O_y$ glass melted at 1250°C in air.

The $T_g$ and $T_x$ temperature for this system are 390°C and 466°C respectively. We note that the exothermic peak appears at 780°C in the bulk sample. It is of particular interest to clarify the origin of this exothermic peak because the $Bi_2Sr_2Ca_2Cu_3O_x$ phase precipitates and grows above this exothermic temperature. It is clear that the reaction among the $Bi_2Sr_{3-x}Ca_xO_y$ (x = I), CuO and $Bi_2Cr_2CuO_x$ phases in the interior of the sample occurs around 780°C.

Fig. 8 shows the temperature dependence of electrical resistance of $Bi_{1.68}Pb_{0.32}Ag_{0.6}Sr_{1.73}Ca_{1.85}Cu_{2.85}O_y$. It is evident that the material exhibits a semiconducting behavior. In fact, the doping of silver in our samples decreases the $T_c$ (0), which varied from 109 to 7K with (x = 0.0 – 0.6).

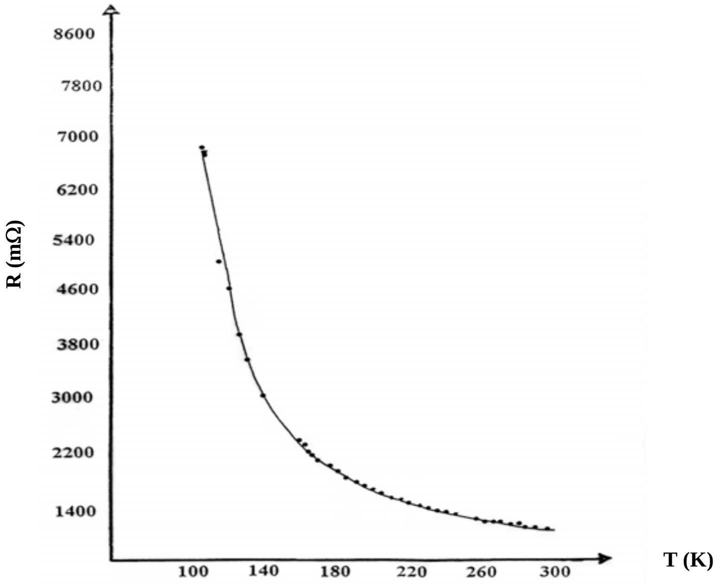

**Fig. 8:** Temperature dependence of resistance for $Bi_{1.68}Pb_{0.32}Ag_{0.6}Sr_{1.73}Ca_{1.85}Cu_{2.85}O_y$.

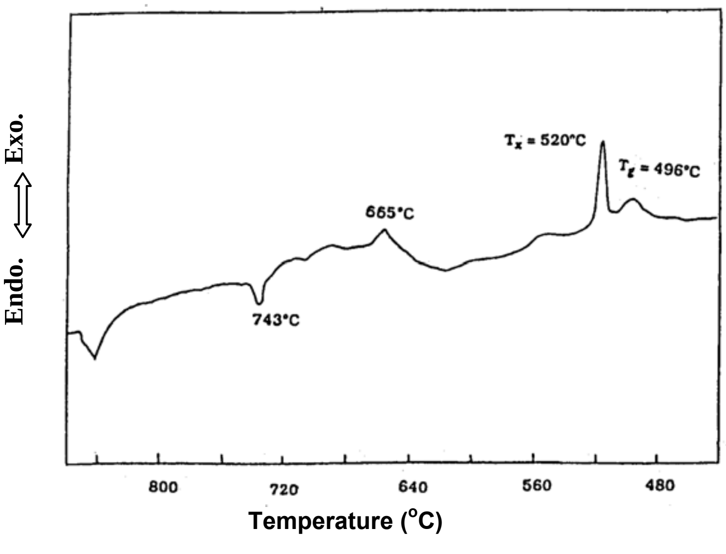

**Fig. 9:** DTA of $Bi_{1.68}Pb_{0.32}Sr_{1.75}Ca_{1.85}Cu_{2.85}O_y$ glasses melted at 1250°C.

The DTA curve (Fig. 9) of the polycrystalline material showed that the glass transition temperature was about 496°C and crystallization temperature was 520°C. The liquid temperature of the glass is about 860°C.

## CONCLUSIONS

Following conclusion can be drawn from the present work:

i. The critical current densities of silver sheathed tapes using the powder-in-tube were found to be in the range I7 x I0$^{8}$ A m$^{-2}$.
ii. Explained on the basis of flux pinning, microstructure and grain growth.
iii. Bi-2223 conductors doped with Sm, Tb, Nb and Ag, their $T_c$, activation energy, critical current density, volume fraction is explained on the basis of possible variation of the hole concentration with trivalent rare earth ion substitution and also by considering the magnetic nature of the substituted ion in the composition.

**Acknowledgements**

Authors thank the Ministry of Sciences, Academy of the Republic of Kazakhstan and Ministry of Sciences and Technology, Government of Pakistan and BICC General, Energy Technology Center, Wreexham, U.K. for funding this program and GIK Institute of Engineering Sciences and Technology for its support.

### References

Azzouz, F. Ben, Chirgui, A.M., Yangui, B., Baulesteix, C. and Salem, M. Ben (**200`**) *Physica*, C 356, 83.

Bansal, N.P. and Doremus, R.H. (**1984**) *J. Thermal Anal.*, 29, 115.

De-Guire, M.R., Bansal, N.P. and Kim, C.J. (**1990**) *J. Amer-Ceram. Soc.*, 73, 1165.

Khan, M.N. and Khizar, M. (**1999**) *J. Mat. Sci.*, 34, 5833.

Khan, M.N., Kayani, A.N. and Haq, A.-ul, (**1998**) *J. Mater. Sci.*, 33, 2365.

Khan, M.N., Khizar, M. and Mukashev, B.N. (**2001**) *Physica*, B 321, 257.

Khan, M.N., Memon, A. and Al-Dalal, S. (**1994**) *Physica*, C 235-240, 491.

Marti, F., Grasso, G., Grivel, J.C. and Flükiger, R. (**1998**) *Supercond. Sci. Technol.*, 11, 485.

Watanab, K. and Kojima, M. (**1998**) *Supercond. Sci. Technol.*, 11, 391.

Wu, M. *et al.* (**1987**) *Phys. Rev. Lett.*, 58, 908.

Zakaullah, Kh., Khan, M.N., Baber, Shaista and Ahmed, Tauseef (**2005**) *Proceedings of 9th ISAM*, Islamabad.